Engineering small tubes with changes in diameter for the study of kidney cell organization

Bastien Venzac, Randa Madoun, Taous Benarab, Sylvain Monnier, Fanny Cayrac, Sarah Myram, Ludovic Leconte, François Amblard, Jean-Louis Viovy, Stephanie Descroix, et al.

Engineering small tubes with changes in diameter for the study of kidney cell organization

Bastien Venzac,[1,2] Randa Madoun,[1,2] Taous Benarab,[1,2] Sylvain Monnier,[1,2,3] Fanny Cayrac,[1,2] Sarah Myram,[1,2,4] Ludovic Leconte,[5] François Amblard,[1,2,6] Jean-Louis Viovy,[1,2] Stéphanie Descroix,[1,2,a),b)] and Sylvie Coscoy[1,2,4,a),b)]

[1]*Laboratoire Physico Chimie Curie, Institut Curie, PSL Research University, CNRS UMR168, 75005 Paris, France*
[2]*Sorbonne Universités, UPMC Univ Paris 06, 75005 Paris, France*
[3]*Univ. Lyon, Université Claude Bernard Lyon 1, CNRS, Institut Lumière Matière, F-69622 Villeurbanne, France*
[4]*Equipe labellisée «Ligue contre le Cancer», Paris, France*
[5]*Institut Curie, PSL Research University, CNRS UMR 144, 75005 Paris, France*
[6]*Center for Soft and Living Matter, Institute for Basic Science (IBS), Departments of Bioengineering and Physics, Ulsan National Institute of Science and Technology, Ulsan, South Korea*

Multicellular tubes are structures ubiquitously found during development and in adult organisms. Their topologies (diameter, direction or branching), together with their mechanical characteristics, play fundamental roles in organ function and in the emergence of pathologies. In tubes of micrometric range diameters, typically found in the vascular system, renal tubules or excretory ducts, cells are submitted to a strong curvature and confinement effects in addition to flow. Then, small tubes with change in diameter are submitted to a local gradient of shear stress and curvature, which may lead to complex mechanotransduction responses along tubes, and may be involved in the onset or propagation of cystic or obstructive pathologies. We describe here a simple method to build a microfluidic device that integrates cylindrical channels with changes in diameter that mimic *in vivo* tube geometries. This microfabrication approach is based on molding of etched tungsten wires, which can achieve on a flexible way any change in diameter in a polydimethylsiloxane (PDMS) microdevice. The interest of this biomimetic multitube system has been evidenced by reproducing renal tubules on chip. In particular, renal cell lines were successfully seeded and grown in PDMS circular tubes with a transition between 80 μm and 50 μm diameters. Thanks to this biomimetic platform, the effect of the tube curvature has been investigated especially regarding cell morphology and orientation. The effect of shear stress on confluent cells has also been assessed simultaneously in both parts of tubes. It is thus possible to study interconnected cell response to differential constraints which is of central importance when mimicking tubes present in the organism.

INTRODUCTION

Tubes are fundamental in the development and functioning of organisms.[1–3] In organs such as kidney, intestine, liver, mammary gland, and in vascular systems, tubes formed with epithelial or endothelial cells surround a fluid-filled lumen undergoing permanent or pulsatile flow. Tubes often exhibit changes in diameter, either physiologically or in a pathological context; it is expected that these changes in diameter lead both to changes in hydrodynamic properties

[a)]S. Descroix and S. Coscoy contributed equally to this work.
[b)]Authors to whom correspondence should be addressed: stephanie.descroix@curie.fr and sylvie.coscoy@curie.fr

(shear stress) and confinement and curvature along the tube. A widely studied example of change in diameter consists in branching in the vascular system or lung.[1,4] Here, we focus on changes in diameter without branching, which are a widespread feature in the organism. These geometries are, for instance, observed at the level of the epithelium of the renal tubule with highly reproducible transitions between the proximal or distal tubule and the Henle loop, with lumen diameters between 50 and 15 μm.[5] In some renal pathologies, defects appear more often at these sites of physiological change in diameter. In nephropathies like nephronophthisis or medullary cystic kidney disease, cysts are predominantly found at corticomedullary junctions, which correspond to sites of physiological change in diameter between the Henle loop and proximal/distal tubule.[6,7] Moreover, in the organism, numerous disorders result in pathological local narrowing or dilatation of tubes, and these acquired tubular shapes lead to subsequent alteration of tissue organization and to additional deformations. These defects are frequently caused by aberrant mechanotransduction, leading to altered proliferation and planar polarity.[8–11]

The topology of tubes (diameter, bending, and branching) is strongly involved in setting the hydrodynamic properties of the lumen flow and hence in inducing cell mechanotransduction responses. Tube topology also influences its own multicellular organization, in particular for the smallest tubes (in the range of 100 μm in diameter) due to confinement and curvature effects. Such micrometric tubes are for example found in renal tubules, vascular and lymphatic system, bile canalicules, mammary, seminal or salivary ducts. In the literature, even in the absence of flow, confinement in meso-scale regions leads to a strong effect on multicellular organization, particularly concerning cell orientation, cytoskeleton organization, and migration.[12–17] Specific curvature effects superimpose with these confinement effects: perpendicular F-actin rings are generated when cells are cultured outside small wires,[12] while multicellular dynamics is deeply altered when cells are cultured inside wires.[18] These confinement/curvature effects were studied only for constant diameters, to the best of our knowledge. Besides, flow application has been demonstrated to generate additional effects on cell behavior compared to a static condition. These effects are particularly well known for endothelial cells, which undergo high physiological shear stress leading to strong cytoskeleton remodeling, orientation, and elongation in the direction of flow.[19–21] This effect of orientation under flow is less well described for epithelial cells, which undergo much lower flow values, although flow leads here to cytoskeleton reorganization[22,23] and orientation of the division axis during renal development.[24]

Because the topologies of tubes, together with their mechanical characteristics, (flow, rigidity) are central in organ function and in the emergence of pathologies, reproducing them in a biomimetic system is crucial to decipher their developmental and pathophysiological mechanisms. Compared to the widely used technique of microlithography, which yields channels with a rectangular section, circular tubes will reproduce the effects of curvature described for epithelial cells at small diameters and avoid differential adhesion for cells in the corners. Moreover, this geometry yields uniform shear stress whatever the position on the section, compared to the varying shear stress in channels with rectangular sections,[25,26] which may have major consequences in studies where collective cell behavior may result from local change in shear stress, as demonstrated in studies on tube dilatation or cyst formation. Many methods were developed in order to mimic the multicellular tube system (reviewed in Ref. 27) relying on either decellularized supports, chip microengineering, 3D printing and two-photon photopolymerization, or generation of hollow fibers.[28,29] Classical lithography techniques allow branching studies but generate channels with a rectangular-shaped section that are not adequate for reproducing the tube circular geometry. Several methods were reported to build simple small circular channel inside PDMS (polydimethylsiloxane) or the hydrogel matrix material. The first technique consisted of gelling or curing the matrix around either glass capillaries, metallic rod or wires.[18,27,30–32] Direct fabrication of hollow fibers was also proposed.[28,29] Beyond generation of simple tubes with a constant section, different approaches were proposed for the generation of more complex networks of circular tubes. A technique based on molding on semi-circular gelatin tubes was proposed for the engineering of branched circular tubes, however, the assembly process would not be adapted to small tube generation.[33] Elegant methods based on sacrificial 3D-printed circular branched sugar alcohol isomalt, or molded sodium alginate lattices,

produced a complex network of cylindrical channels.[34,35] Direct methods based on 3D printing or two-photon photopolymerization[36–38] theoretically allow to draw any network with circular tubes, however the resolution of 3D printing is still not completely compatible with the smallest tubes, and two-photon photopolymerization remains a technique not widely accessible (because it is costly and time consuming).

The combination of confinement/curvature and flow constraints on epithelial cells in non-uniform topographies with change in diameter has not been investigated yet. Reproducing a change in diameter in a single tube is important for pathophysiological studies, because (1) it will give the information (cell morphology, function, signaling) on what is happening in the transition region between two confined zones of different geometrical characteristics and (2) upon flow generation, it will ensure that different tube parts are subjected to the same input flow rate. Here, we propose a simple approach to produce a microfluidic device containing multicellular micrometric tubes with change in diameter that mimic renal tubes' geometry. This approach relies on a technique of molding of etched wires in a PDMS matrix and gives access to a wide range of changes in diameters. To demonstrate the potential of our biomimetic approach, we investigate the organization of renal epithelial MDCK (Madin-Darby Canine Kidney) cells in PDMS circular channels with a change in diameter from 80 to 50 μm, which corresponds to a lumen diameter of 65 to 35 μm, close to physiological conditions. In particular, thanks to this microfluidic platform, we studied cellular changes in orientation and elongation along the tube due to confinement/curvature gradients, and the response to flow generation. This method will pave the way to studies aiming at deciphering how coupled effects of gradients of shear stress and curvature are managed by mechanotransduction systems (e.g., ion channels, adhesion molecules), in multicellular tubes with changes in diameter characteristic for physiological or pathological conditions.

EXPERIMENTAL

Microfabrication

Circular channels were fabricated by the removal of etched tungsten wires from a polydimethylsiloxane (PDMS) piece. First, tungsten wires (Goodfellow) with a diameter of 80 μm were half-varnished with nail polish (Clinique). The polish brush was mounted on a translational stage for a better control of the nail polish deposition. The polished wires were immerged and shaken during 8 h in 10 μl of Murakami's etchant, containing 0.13 g of KOH, 0.34 g of KH_2PO_4, and 0.33 g of $K_3Fe(CN)_6$ (Sigma) in order to reduce the diameter of the exposed part of the wire. The nail polish was then removed with acetone.

The etched tungsten wires were inserted through two 1 mm-wide holes, 5 mm apart, created on a microscopic glass slide (26 $\times$ 75 mm, VWR) by abrasive blasting through a drilled steel mask. Up to 8 wires were put in parallel on the same glass slide. The diameter change was located between the two holes. PDMS (Sylgard 184, Dow Corning), mixed at a 10:1 ratio with the curing agent, was then poured on the glass slide and cured during 2 h at 70 °C. The tungsten wires were removed from the PDMS and access inlets (2 mm in diameter) were punched at the position of the previous holes. The PDMS part was finally bonded to a circular cover slip (32 mm, 0.17 mm) with a plasma treatment.

Cell culture and flow experiments

MDCK cells were cultured in DMEM (Dulbecco's Modified Eagle's Medium) supplemented with 10% FCS (Fetal Calf Serum), at 37 °C and 5% CO_2. MDCK Lifeact-GFP cells were obtained by stable transfection with Lifeact-GFP plasmid (Ibidi) as previously described.[12,39] E-cadherin-DsRed MDCK cells were kindly given by Nelson,[40] MDCK Fucci cells were a kind gift of Hufnagel.[41] Stable Lifeact-GFP transfected cells were grown in complete media with 0.4 mg/ml geneticin (Invitrogen).

Before cell seeding, circular channels were first sterilized in ethanol and rinsed with PBS (Phosphate-Buffered Saline). They were afterwards coated, either with fibronectin (Sigma Aldrich; 1 h room temperature, 50 μg/ml in PBS) or laminin or type IV collagen (Sigma

Aldrich, respectively, 100 μg/ml and 30 μg/ml in PBS 2 h at 37 °C) and rinsed again in PBS. A drop of filtrated, concentrated cells (1–5 $\times$ 10^6 of cells in 100 μl of complete media) was deposited on one side of the channel with a 10 μl Hamilton syringe. Hydrostatic flows moved the cell suspension through the channel and cells sedimented randomly in the channels and reservoirs. After 1 h, the media was changed and the cells attached at the bottom of the reservoirs were mechanically detached and aspirated.

An initial 1-day adhesion without flow at 37 °C was performed; afterwards, either flow was applied for one day (for flow experiments), either medium was changed once or twice a day in the channels (for static experiments).

For flow application, the microfluidic chip was kept during 1 day in an incubator at 37 °C and 5% CO_2, with the complete MDCK culture medium pushed by a syringe-pump (either Harvard Apparatus or Aladdin, World Precision Instruments) at a flow rate of 0.15 μl/min.

Labeling and imaging

Cells were either imaged alive (Lifeact-GFP or cadherin-DsRed MDCK cells), or fixed in tubes with 4% paraformaldehyde in PBS (WT (Wild-Type) MDCK cells). F-actin was labelled on MDCK WT cells with 25 μg/ml phalloidin-TRITC (tetramethylrhodamine isothiocyanate) (Sigma); labeled structures were conserved and imaged in PBS without the mounting step.

The images were acquired—on a spinning disk microscope (Gataca Systems, France). The spinning disk microscope is based on a CSU 22 Yokogawa head mounted on an inverted Ti-E Nikon microscope equipped with a motorized XY Stage. The images were acquired through a 40$\times$ 1.4 NA CFI Super Plan Fluor ELWD objective with a EMCCD camera (QuantEM, Photometrics, USA). Optical sectioning was achieved using a piezo stage (PIFOC Nanopistionners, PI, France). Gataca Systems' laser bench is equipped with 405, 491, and 561 nm laser diodes, delivering 100 mW each, coupled to the spinning disk head through a single-mode fiber. Multi-dimensional acquisitions were performed in the streaming mode using the Metamorph 7.7.6 software (Molecular Devices), or—on a spinning disk CSU-X1–1.000 rpm (Leica), Hamamatsu Flash 4V2 cameras, 40$\times$ or 10$\times$ objectives (Imaging facility of Institute Pierre-Gilles de Gennes).

Image analysis

Images were treated and analyzed with ImageJ or Metamorph (Meta Imaging Series) (z projections, enhancement of contrast or denoising for graphical representation). For denoising, Safir Filter ImageJ plugin developed by Jerome Boulanger was used.[42] Cell length and angle with the tube direction (between 0° and 90°) refer to manual measurements on the cell long axis. The width was measured on the cell perpendicular short axis, with the inverse aspect ratio defined as the ratio between the length of the short axis and the length of the long axis. Measurements were done with ImageJ. The measurements of individual cells orientation were confirmed by measurements of local orientation performed with OrientationJ (written by Daniel Sage, EMBL)[43] (not shown). The relative proportions of red and green Fucci cells (approximated as proportions of red and green areas) were computed after binarization and surface area measurement in each image. The graphs were plotted with Kaleidagraph, and statistical analysis (Student's t-test) performed with Microsoft Excel.

RESULTS AND DISCUSSION

Microfabrication of biomimetic tubes with changes in diameter

To study the influence of geometry and shear stress on an epithelial monolayer, we developed an original approach to generate tubes with diameter changes in a PDMS matrix as support for cell culture. The microfabrication process was designed to fulfill several requirements. First, it should produce an array of circular channels with changes in diameter with dimensions in the same order of magnitude than *in vivo*, here in particular, we aim at reproducing renal tubes. Second, the technology should be compatible with high-resolution imaging. It implies that the distance between the tubes and the coverslip had to be small enough (below mm).

Finally, for easy handling in biological labs, solution injection for coating, washing and cell seeding should be simply made by pipetting.

In order to build micrometric tubes in PDMS with changes in diameter, we first generated cylindrical wires with a discontinuous diameter. To do so, we used chemical etching with wires partially protected to limit the etching zone. This heterogeneous etching was made possible by varnishing half of the tungsten wires. To achieve a sharp transition in diameter, we optimized the varnishing step so that a thin and uniform film of nail polish covered partially the wire by dip coating. Then, a Murakami's etchant was used to slowly etch the unprotected tungsten wire side, from 80 μm to 50 μm. A reproducible and progressive change in diameter is obtained, with a typical angle of 45° due to the isotropic etching. The microdevice fabrication is reported in Fig. 1. Briefly, wires were then inserted in a drilled glass slide and a mix of liquid PDMS and curing agent was poured above the glass slide. After curing, the wires were easily removed without any lubricant and their shapes were directly transferred into the PDMS. Importantly, this technique created channels close (typically 200–400 μm) to the glass coverslip for imaging with working distances associated with high resolution objectives. The number of circular channels per chip was fixed at 6.

To promote cell adhesion to the PDMS circular channels, coating of the lumen with fibronectin, or laminin or collagen IV corresponding to extracellular matrix physiologically present in renal tubules, was performed by a simple injection into the channels. As assessed by fluorescent laminin coating, this approach resulted in homogenous coating uniform along channels (data not shown). We thus demonstrate the possibility to simply inject cell suspensions within the channels and show similar adhesion and morphologies for the three different coating molecules.

In our set-up, tube colonization did not start from the reservoirs. Instead, cell colonization originated from initial random areas of cell adhesion inside tubes, which were distributed quite evenly between the different sections. This procedure avoided any bias that would result from colonization from one particular side (small or large diameter). To take into account a possible heterogeneity between the different experiments, we systematically confirmed our conclusion by checking that the observed results (difference small/large) were identical in all pairs of different segments of tubes. We also checked that our angle measurements were largely independent on cell sizes (linked to cell density) among the different experiments (see supplementary material).

Renal epithelial cells form confluent epithelia in tubes

Renal MDCK were used as an epithelial cell model to reconstitute the renal tube with change in diameter. The choice of this classical model of tubular cell line of distal origin as a proof of concept represents a first step towards more complex models that could recapitulate in particular, the different cell types present *in vivo* in the different parts of the tubules: proximal tubules (diameter 50 μm, cuboidal cells with developed brush border), thin descending and ascending Henle loops (diameter 15 μm, flat, squamous epithelial cells), thick ascending part of the Henle loop (cuboidal cells with extensive basal invaginations), and distal convoluted tubules (diameter 30–40 μm, cuboidal cells). Seeding in our tubes with change in diameter between 80 μm and 50 μm led to a lumen diameter around 65 and 35 μm, close to the *in vivo* situation. Dimensions were selected to achieve a trade-off between the *in vivo* situation (50 and 15 μm) and ease of cells seeding. Renal epithelial MDCK cells seeded in channels with diameter between 80 and 50 μm were able to form a confluent epithelium, colonizing either wide regions of the channels (generally >300 μm long) or the whole tube (depending on seeding conditions) after 1 day in culture. Cells could be cultivated several days in tubes, providing a daily change in media was performed with pipetting. Figure 2(a) shows a tube uniformly covered with Lifeact-GFP MDCK cells, 8 days after seeding. To further assess the biocompatibility of our tube chip approach, cell survival was systematically checked through the continuous production of Lifeact-GFP. It was also monitored with MDCK-Fucci cells,[41] showing that about 30% cells were in the S/G2/M phase indicative of a progression in the cell cycle and 70% in the quiescent

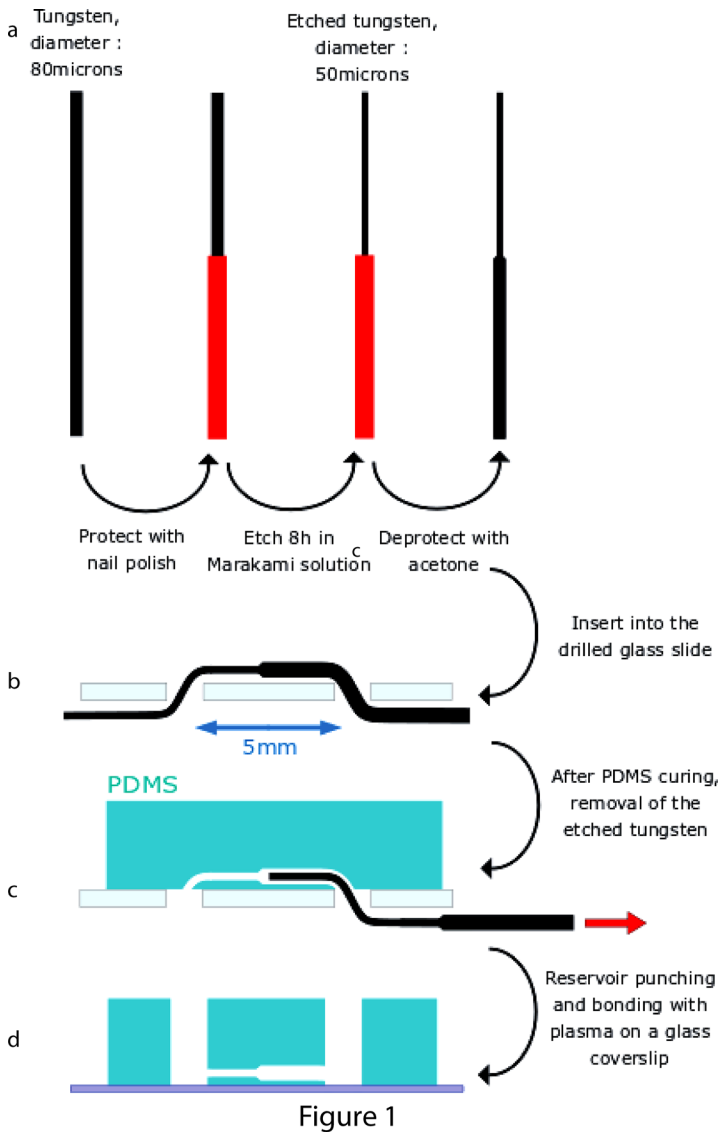

Figure 1

FIG. 1. Schematic representation of the microfabrication process. (a) Tungsten wires with controlled change in diameter were generated by etching with partial protection of the wire. (b) Half-etched tungsten wires were inserted into a drill glass slide. (c) Removal of the tungsten wires after PDMS curing created tubes with change in diameter. (d) The PDMS part was removed from the previous glass slide, reservoirs were punched, and the PDMS device was bounded to a glass coverslip by plasma treatment.

G0 or G1 phase after 2–3 days culture [Fig. 2(b)]. These proportions were similar to cells in 2D cultures in our experimental conditions, suggesting that cells culture in channels did not affect cells cycle progression. High-resolution imaging showed that confluent cells established inter-cellular contacts rich in F-actin in each part of the tube, thanks to a Lifeact-GFP labeling on live cells [Figs. 2(c)–2(e)]. We also evidenced an adequate formation of *adherens* junctions between cells by E-cadherin-GFP stable expression [Fig. 2(f)]. Together, these observations demonstrate that our approach is able to reconstitute a confluent monolayer of renal cell lines in circular channels of small sizes over several days.

Cell organization and morphology as a function of the tube diameter

To further investigate cell behaviors as function of the tube geometry, we defined three zones of interest in these tubes: (i) large diameter, (ii) change in diameter (including cells partly present

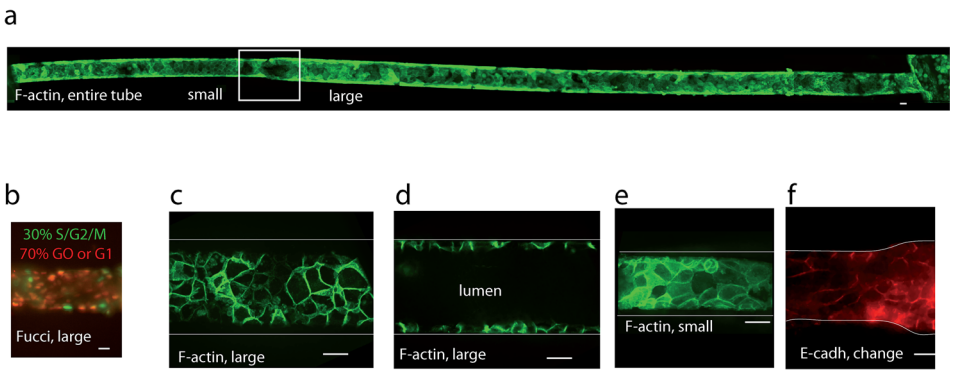

FIG. 2. Characterization of cells in tubes with change in diameter. (a) Long-term culture in tubes. Imaged with a 10× objective at spinning disk, z projection, and concatenation of images to get the whole tube. MDCK Lifeact-GFP cells were seeded in circular PDMS fibronectin-coated tubes with change in diameter (square) between 50 μm (right) and 80 μm (left). They were maintained in culture for 8 days (shown here), with uniform confluency in the whole tube obtained before day 2. Culture conditions were here sequentially: static conditions for 2 days, flow (0.15 μl/min) for 1 day, and static conditions for 5 days. All other subfigures refer to shorter-term culture (3-5 days) without flow. (b) MDCK-Fucci cells in laminin-coated tube, 3 days culture. (c) MDCK Lifeact-GFP cells in tubes (large section), coated with fibronectin, 5 days culture: z projection of the lower half of the tube, or (d) profile view. (e) MDCK Lifeact-GFP cells in a small section, same conditions as (c) and (d). (f) MDCK-E-cadherin-DsRed cells in collagen-coated tubes, 3 days culture, change in diameter (z projection). The bar represents 20 μm. (c)–(f) Imaging with ×60 objective at the spinning disk.

in this region), and (iii) small diameter. In order to assess the influence of cell curvature and confinement on the morphology first in static conditions, cell dimensions and orientations were quantified in these different zones of tubes [Fig. 3(a), Table I]. This was done by manual measurements, for all cells, of angles of the cell principal axis with the tube direction. The most important feature was an increase in orientation (defined as the angle with tube direction) in the small diameter section compared with the large diameter section. In the large diameter section, the angle distribution (between 0° and 90°) is almost random (orientation slightly biased toward the tube direction), as reflected by its mean value of 37°, close to 45° corresponding to random orientation. In the small diameter section, angle values are shifted to 0, with a mean angle of 28°, which illustrates an increased alignment in the tube direction. [Fig. 3(a), Table I, statistically significant difference with $p < 10^{-4}$, $n = 386$ and 440 cells]. This tendency was systematic in each pair of small- and large-sections in the same tube, for fibronectin-coated tubes corresponding to the reported statistics, as well as in collagen IV-coated tubes (n cells = 85, not shown). Orientation in the "change of diameter" region appears intermediate. Increased orientation in the small part is summarized in Fig. 3(b). The change in orientation was the most striking difference between large and small parts, while differences in cell shape factors like elongation (here estimated from the cell inverse aspect ratio), were less significant.

The observed increase in orientation in the small section is in the range of the effects reported in experiments on MDCK cells confined on 2D tracks, with a change from random orientation to a partially oriented morphology for small widths.[17] Our results are in agreement with these effects imposed by confinement, i.e., an increase in orientation significant but of relatively low magnitude, progressively in the range of 80–50 μm. Curvature effects potentially superimpose here on confinement effects but both cannot be disentangled in these conditions. These combined effects of confinement and curvature were studied for endothelial cells in capillaries of different diameters, or epithelial MDCK cells without flow, for which an increase in orientation and elongation has been shown for the same range in diameters.[18,44] These curvature effects were studied in detail for MDCK cells in a report with individual tubes of different diameters, with similar reported effects of progressive increased cell and F-actin orientation for a diameter inferior to 75–100 μm for MDCK cells in tubes, combined to decreased migration at these diameters, reflecting both local effects on cytoskeleton/adhesion mechanical organization and long-range intercellular effects for small diameters at strongly negative curvatures.[18] This effect is important for the field of collective behaviour; physiologically, the effects of constant

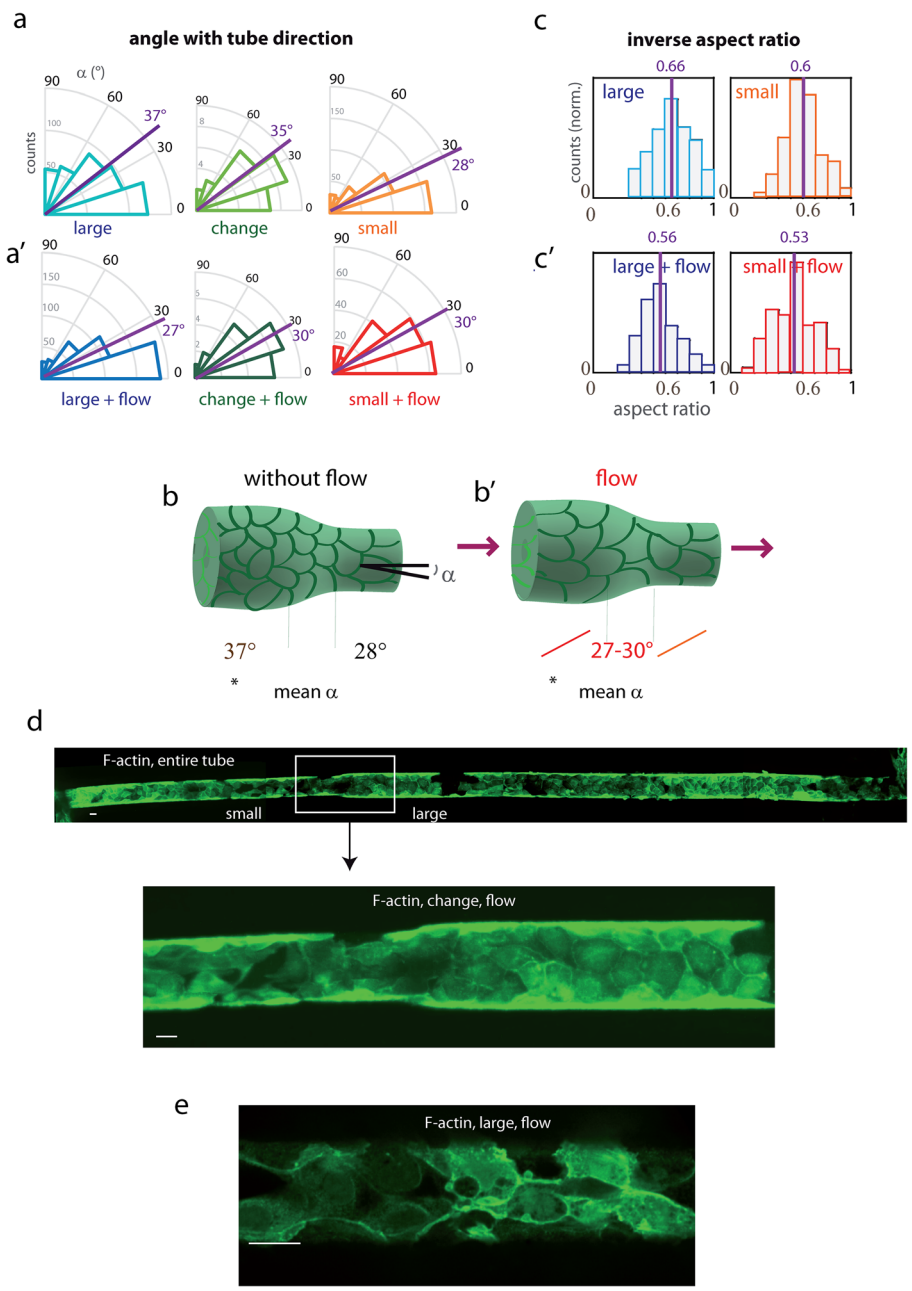

FIG. 3. Orientation and elongation of cells in tubes with or without flow. (a) Cell orientation and elongation in the different tube parts: (a) angles with the tube axis of the cell principal direction, measured in the different parts of tubes: large-diameter (blue), change in diameter (green), and small-diameter (orange). All measurements were made in fibronectin-coated tubes, 3–5 days after cell seeding. Large and small-diameters data were statistically significantly different with $p < 10^{-4}$ (see Table I). Mean angles are indicated in magenta. (a′) Similar diagrams after one day of continuous flow (0.15 μl/min). (b) and (b′) Recapitulative scheme of orientation as a function of tube diameter, in static conditions (left) and under flow (right). (c) and (c′) Histograms of the inverse aspect ratio (length of short axis divided by the length of the long axis) (c) in static conditions: large-diameter section (blue), small-diameter section (orange), and (c′) after 1 day of continuous flow: large-diameter section (dark blue), small-diameter section (red). Counts (y axis) were normalized so that the histogram area was the same for the different conditions. See Table I for statistics. (a to c′) Organization in the large-diameter section in static conditions systematically differed from other conditions, with statistically significant differences, $p < 10^{-4}$. Mean ratios are indicated in magenta. (d) Whole-tube image of MDCK Lifeact-GFP cells in the fibronectin-coated tube upon flow (0.15 μl/min). Imaging performed at the spinning disk with a $\times 10$ objective (top, concatenated fields, bottom, detail). After seeding, the cells were kept 2 days in static conditions in order to achieve optimal binding, and a 1-day flow was applied. (b) zoom on the region of change in diameter. The bar represents 20 μm. (e) F-actin organization (Lifeact-GFP labeling, lower part of the tube) after 1-day flow, imaged with a 60$\times$ objective, spinning disk.

TABLE I. Statistics on cell organization. Statistics in the different parts of fibronectin-coated tubes, without and with flow (0.15 μl/min for 1 day), are shown: mean, standard deviation, number of cells; in No. of tubes = 8 (without flow), 4 (flow on tube with change in diameter), plus 4 (flow in tube with constant flow). "*stat diff from*" indicate conditions with which a statistically significant difference with $p < 10^{-4}$ was determined. Boldface values refer to mean values, italic values to indications about conditions with statistically significant differences.

	Large, *l*	Change, *c*	Small, *s*	Large-flow, *l-f*	Change-flow, *c-f*	Small-flow, *s-f*
Angle (deg)						
Mean	**37.3**	**35.3**	**27.8**	**27.3**	**30**	**30.5**
Standard deviation	25.9	21.8	24	23.3	21.9	22.4
No. of cells	440	39	386	438	21	192
Stat. diff. from	*s, l-f*		*l*	*l*		
Inverse aspect ratio						
Mean	**0.66**	**0.61**	**0.6**	**0.56**	**0.53**	**0.53**
Standard deviation	0.16	0.15	0.14	0.16	0.13	0.17
No. of cells	312	24	401	346	15	152
Stat. diff. from	*l-f*		*s-f*	*l*		*s*
Length (μm)						
Mean	**20.7**	**18.6**	**17**	**27.8**	**27.7**	**26.2**
Standard deviation	5.9	3.5	7.8	8.8	8.4	8.4
No. of cells	287	24	400	412	15	152
Stat. diff. from	*l-f*		*s-f*	*l*		*s*

luminal flow have to be superimposed. Physiologically, an adequate planar polarity is important for maintaining the tube diameter during proliferation events, in particular tubular elongation during development[24] or in epithelial repair events. Here, thanks to this original microfabrication approach, the study of geometrical transitions and the coupling between regions of different diameters has been made possible on chip.

EFFECT OF FLOW ON CELL ORGANIZATION IN TUBES

Tubes with changes in diameter give rise to spatial variations of shear stress with a constant input flow. We generated flows of low magnitude on cells in tubes (1 day flow at 0.15 μl/min after 2 days in static conditions) [Figs. 3(d) and 3(e)]. This is in the range of values found *in vivo* in renal tubules [shear stress values of 0.2-1 dyn cm^{-2}].[22,49] Changes in orientation and elongation generated by flow were thus investigated. In a large diameter section, orientation increased upon flow, compared to the absence of flow, with the angle direction shifting from mean values of 37.3° to 27.3° (n = 440 and 438 cells, statistically significant difference) [Figs. 3(a) and 3(a′), Table I]. Cells became also more elongated, with the inverse aspect ratio from 0.66 to 0.56 [Figs. 3(c) and 3(c′)], and longer (length of the cell long axis from 20.7 μm to 27.8 μm) (Table I). In contrast, in small-diameter tubes, orientation remained largely unchanged (mean angle value from 27.8° to 30.5°, n = 386, 192), while cells slightly elongated with the inverse aspect ratio shifting from 0.6 to 0.53 [Figs. 3(a) and 3(a′), Table I], reaching values similar to the large-diameter part. The part with change of diameter, which exhibited without flow an orientation intermediate between large and small parts, oriented upon flow to reach values similar to the surrounding large and small parts (mean angle value shifting from 35.3° to 30°), also with a similar elongation. These results show that under shear stress, the cellular organization became uniform in the whole tube whatever the channel diameters, and cells oriented similar to cells in the small-diameter section without flow. Figures 3(b) and 3(b′) illustrate this homogenization of orientation upon flow. Physiologically, the cell types in the different parts of the tubule have very different morphological and functional properties (although the morphology or cell division axis being reported non isotropic towards tube axis in several studies for different types).[24,45,46] Orientation and elongation under flow are well known for endothelial cells, however reorientation and elongation of cell shape observed here in large diameter were not described in 2D studies for epithelial cells. For

epithelial cells in *in vitro* culture, cytoskeleton reorganization including reinforcement of peripheral focal contacts and actin bundles were described upon prolonged flow, and are essential for the maintenance of epithelial integrity.[22,47,48] Analysis of the cytoskeleton and contact reorganization goes beyond the scope of this paper, however, one could imagine that cells in small diameter already have a cytoskeletal reinforcement at the periphery because of increased confinement, and may be therefore less sensitive to flow as in large diameter. On a very hypothetical way, one could imagine that homogenization of orientation by flow for a given cell type would render cells less sensitive to the change in diameter (e.g., tube dilatation), allowing to keep planar polarity despite changes in curvature constraints; such properties may be lost for cells with altered mechanotransduction (e.g., ADPKD, nephronophthisis).[24]

CONCLUSION

Methods of circular tube generation by molding were described in the literature, however, to the best of our knowledge, it has been limited so far to tubes with a constant diameter.[18,30,31] Our system allows to generate a change in diameter with circular tubes, and to reproduce geometry and precise flows observed in tubes of varying section in the organism. The system is very versatile and allows virtually any change of diameter, or successive sections of varying diameter, by adapting the protected areas on a tungsten wire, and the duration of etching. Here, small diameters were chosen in order to approach physiological conditions (e.g., kidney tubules), and also because confinement effects are expected in this range.

Thanks to this unique platform, we showed that a uniform covering of epithelial confluent cells could be obtained and maintained for a long-term cell culture, even in small PDMS channels (up to two weeks). We illustrated the potential of our method by studying the effects of diameters and flow on epithelial cell orientation. We observed an increase in cell orientation toward the tube axis, in agreement with the literature concerning confinement, with mild transitions for the change in diameter area. Moreover, different effects of flow in function of diameter were observed (orientation and elongation in large-diameter, no or minimal effect in small diameter), leading to homogenization of orientation upon flow in the different regions.

Directions to improve our system in order to go closer to physiological and pathological conditions would include: (1) seeding large and small diameters with different cell types (e.g., proximal tubule/Henle loop), for example, by sequential seedings, with removal of only half of the wire before the first seeding, (2) comparing physiological flows with increased flows observed in pathological conditions: indeed, in a wide number of chronic nephropathies, obstructions in some nephrons leads to hyperfiltration in the remaining functional nephrons, with an increased flow rate value, which can reach a factor 2–4.[49] On a physiological side, applying a pulsatile flow may also be important, as it has been described physiologically (frequency 1–5 Hz) and will modulate cell mechanotransduction response.[50]

Below these specific conditions, this system could be used for a variety of situations where particular effects could be expected at the region of change in diameter. This system could be used for the study of diseases where variations in tube diameters play important roles, in particular in kidney (like nephronophthisis, where cysts are more concentrated in corticomedullary junctions that could correspond to areas of transitions with the Henle loop). Moreover, this system could also be used directly for the study of other types of multicellular, epithelial tubes (lymphatic vessels, mammary glands, etc.,) by changing the cell type seeded and the tube dimensions.

SUPPLEMENTARY MATERIAL

See supplementary material for details about the seeding procedure and relationship between cell angles and characteristic sizes.

ACKNOWLEDGMENTS

We are very grateful to Sophie Saunier, Fabiola Terzi, Marco Pontoglio, Laurent Malaquin, Alexandre Benmerah, Cécile Jeanpierre, Evelyne Fischer, and Flora Legendre for the insightful

discussions at the origin of this project. We thank very much Pascal Silberzan, Hannah Yevich, Isabelle Bonnet, Victor Yashunsky, and Guillaume Duclos for the important discussions and help with the image analysis. We thank Olivier Cochet for sharing his MDCK Lifeact-GFP cell line, W. J. Nelson for sharing the MDCK-E-cadherin-DsRed cell line, and Lars Hufnagel for sharing the MDCK-Fucci cell line. We greatly acknowledge Anne-Christine Brunet for cell biology, Lucie Sengmanivong of the Nikon Imaging Centre at Institut Curie-CNRS, and François Waharte and Vincent Fraisier from the PICT-IBiSA Lhomond Imaging facility of Institut Curie. This work was sponsorized by the CNRS (Centre National de la Recherche Scientifique), Institut Curie, and ERC CellO. The authors greatly acknowledge the Cell and Tissue Imaging (PICT-IBiSA), Institut Curie, member of the French National Research Infrastructure France-BioImaging (ANR10-INBS-04). This work has received the support of the Institut Pierre-Gilles de Gennes (Equipement d'Excellence, "Investissement d'avenir," Program No. ANR-10-EQPX-34).

[1]D. J. Andrew and A. J. Ewald, "Morphogenesis of epithelial tubes: Insights into tube formation, elongation, and elaboration," Dev. Biol. **341**, 34–55 (2010).
[2]M. M. Zegers, L. E. O'Brien, W. Yu, A. Datta, and K. E. Mostov, "Epithelial polarity and tubulogenesis in vitro," Trends Cell Biol. **13**, 169–176 (2003).
[3]F. Martin-Belmonte and A. E. Rodriguez-Fraticelli, "Chapter 3: Acquisition of membrane polarity in epithelial tube formation patterns, signaling pathways, molecular mechanisms, and disease," Int. Rev. Cell Mol. Biol. **274**, 129–182 (2009).
[4]R. J. Metzger, O. D. Klein, G. R. Martin, and M. A. Krasnow, "The branching programme of mouse lung development," Nature **453**, 745–750 (2008).
[5]M. A. Knepper, R. A. Danielson, G. M. Saidel, and R. S. Post, "Quantitative analysis of renal medullary anatomy in rats and rabbits," Kidney Int. **12**, 313–323 (1977).
[6]R. Salomon, S. Saunier, and P. Niaudet, "Nephronophthisis," Pediatr. Nephrol. **24**, 2333–2344 (2009).
[7]F. Hildebrandt, R. Waldherr, R. Kutt, and M. Brandis, "The nephronophthisis complex: Clinical and genetic aspects," Clin. Invest. **70**, 802–808 (1992).
[8]F. Kotsis, C. Boehlke, and E. W. Kuehn, "The ciliary flow sensor and polycystic kidney disease," Nephrol., Dial., Transplant. **28**, 518–526 (2013).
[9]A. Patel and E. Honore, "Polycystins and renovascular mechanosensory transduction," Nat. Rev. Nephrol. **6**, 530–538 (2010).
[10]V. Patel *et al*., "Acute kidney injury and aberrant planar cell polarity induce cyst formation in mice lacking renal cilia," Hum. Mol. Genet. **17**, 1578–1590 (2008).
[11]T. Weimbs, "Polycystic kidney disease and renal injury repair: Common pathways, fluid flow, and the function of polycystin-1," Am. J. Physiol. Renal Physiol **293**, F1423–F1432 (2007).
[12]H. G. Yevick, G. Duclos, I. Bonnet, and P. Silberzan, "Architecture and migration of an epithelium on a cylindrical wire," Proc. Natl. Acad. Sci. U. S. A. **112**, 5944–5949 (2015).
[13]A. I. Teixeira, G. A. Abrams, P. J. Bertics, C. J. Murphy, and P. F. Nealey, "Epithelial contact guidance on well-defined micro- and nanostructured substrates," J. Cell Sci. **116**, 1881–1892 (2003).
[14]J. N. Hanson *et al*., "Textural guidance cues for controlling process outgrowth of mammalian neurons," Lab Chip **9**, 122–131 (2009).
[15]E. Martinez, E. Engel, J. A. Planell, and J. Samitier, "Effects of artificial micro- and nano-structured surfaces on cell behaviour," Ann. Anat. **191**, 126–135 (2009).
[16]M. Thery, "Micropatterning as a tool to decipher cell morphogenesis and functions," J. Cell Sci. **123**, 4201–4213 (2010).
[17]S. R. Vedula *et al*., "Emerging modes of collective cell migration induced by geometrical constraints," Proc. Natl. Acad. Sci. U. S. A. **109**, 12974–12979 (2012).
[18]W. Xi, S. Sonam, T. Beng Saw, B. Ladoux, and C. Teck Lim, "Emergent patterns of collective cell migration under tubular confinement," Nat. Commun. **8**, 1517 (2017).
[19]C. Hahn and M. A. Schwartz, "Mechanotransduction in vascular physiology and atherogenesis," Nat. Rev. Mol. Cell Biol. **10**, 53–62 (2009).
[20]A. M. Malek and S. Izumo, "Mechanism of endothelial cell shape change and cytoskeletal remodeling in response to fluid shear stress," J. Cell Sci. **109**(Pt 4), 713–726 (1996).
[21]C. K. Thodeti *et al*., "TRPV4 channels mediate cyclic strain-induced endothelial cell reorientation through integrin-to-integrin signaling," Circ. Res. **104**, 1123–1130 (2009).
[22]Y. Duan *et al*., "Shear-induced reorganization of renal proximal tubule cell actin cytoskeleton and apical junctional complexes," Proc. Natl. Acad. Sci. U. S. A. **105**, 11418–11423 (2008).
[23]D. Verma *et al*., "Interplay between cytoskeletal stresses and cell adaptation under chronic flow," PLoS One **7**, e44167 (2012).
[24]E. Fischer *et al*., "Defective planar cell polarity in polycystic kidney disease," Nat. Genet. **38**, 21–23 (2006).
[25]L. K. Fiddes *et al*., "A circular cross-section PDMS microfluidics system for replication of cardiovascular flow conditions," Biomaterials **31**, 3459–3464 (2010).
[26]M. Abdelgawad *et al*., "A fast and simple method to fabricate circular microchannels in polydimethylsiloxane (PDMS)," Lab Chip **11**, 545–551 (2011).
[27]J. G. Nemeno-Guanzon *et al*., "Trends in tissue engineering for blood vessels," J. Biomed. Biotechnol. **2012**, 956345.
[28]T. Nguyen du, Y. T. Leho, and A. P. Esser-Kahn, "Process of making three-dimensional microstructures using vaporization of a sacrificial component," J. Visualized Exp. **81**, e50459 (2013).

[29]N. Diban *et al*., "Hollow fibers of poly(lactide-co-glycolide) and poly(epsilon-caprolactone) blends for vascular tissue engineering applications," Acta Biomater. **9**, 6450–6458 (2013).
[30]M. E. Dolega *et al*., "Facile bench-top fabrication of enclosed circular microchannels provides 3D confined structure for growth of prostate epithelial cells," PLoS One **9**, e99416 (2014).
[31]E. J. Weber *et al*., "Development of a microphysiological model of human kidney proximal tubule function," Kidney Int. **90**, 627–637 (2016).
[32]A. Tourovskaia, M. Fauver, G. Kramer, S. Simonson, and T. Neumann, "Tissue-engineered microenvironment systems for modeling human vasculature," Exp. Biol. Med. **239**, 1264–1271 (2014).
[33]J. He *et al*., "Fabrication of circular microfluidic network in enzymatically-crosslinked gelatin hydrogel," Mater. Sci. Eng., C **59**, 53–60 (2016).
[34]M. K. Gelber and R. Bhargava, "Monolithic multilayer microfluidics via sacrificial molding of 3D-printed isomalt," Lab Chip **15**, 1736–1741 (2015).
[35]X. Y. Wang *et al*., "Engineering interconnected 3D vascular networks in hydrogels using molded sodium alginate lattice as the sacrificial template," Lab Chip **14**, 2709–2716 (2014).
[36]K.-S. Lee, R. H. Kim, D.-Y. Yang, and S. H. Park, "Advances in 3D nano/microfabrication using two-photon initiated photopolymerization," Prog. Polym. Sci. **33**, 631–681 (2008).
[37]S. D. Gittard and R. J. Narayan, "Laser direct writing of micro- and nano-scale medical devices," Expert Rev. Med. Devices **7**, 343–356 (2010).
[38]G. Gao and X. Cui, "Three-dimensional bioprinting in tissue engineering and regenerative medicine," Biotechnol. Lett. **38**, 203 (2015).
[39]S. Coscoy *et al*., "Molecular analysis of microscopic ezrin dynamics by two-photon FRAP," Proc. Natl. Acad. Sci. U. S. A. **99**, 12813–12818 (2002).
[40]T. D. Perez, M. Tamada, M. P. Sheetz, and W. J. Nelson, "Immediate-early signaling induced by E-cadherin engagement and adhesion," J. Biol. Chem. **283**, 5014–5022 (2008).
[41]S. J. Streichan, C. R. Hoerner, T. Schneidt, D. Holzer, and L. Hufnagel, "Spatial constraints control cell proliferation in tissues," Proc. Natl. Acad. Sci. U. S. A. **111**, 5586–5591 (2014).
[42]C. Kervrann and J. Boulanger, "Optimal spatial adaptation for patch-based image denoising," IEEE Trans. Image Process. **15**, 2866–2878 (2006).
[43]R. Rezakhaniha *et al*., "Experimental investigation of collagen waviness and orientation in the arterial adventitia using confocal laser scanning microscopy," Biomech. Model. Mechanobiol. **11**, 461–473 (2012).
[44]M. Ye *et al*., "Brain microvascular endothelial cells resist elongation due to curvature and shear stress," Sci. Rep. **4**, 4681 (2014).
[45]L. W. Welling, D. J. Welling, J. W. Holsapple, and A. P. Evan, "Morphometric analysis of distinct microanatomy near the base of proximal tubule cells," Am. J. Physiol. **253**, F126–F140 (1987).
[46]H. Takahashi-Iwanaga, Y. Iwata, K. Adachi, and T. Fujita, "The histotopography and ultrastructure of the thin limb of the Henle's loop: A scanning electron microscopic study of the rat kidney," Arch. Histol. Cytol. **52**(4), 395–405 (1989).
[47]J. Rahimzadeh *et al*., "Real-time observation of flow-induced cytoskeletal stress in living cells," Am. J. Physiol. Cell Physiol. **301**, C646–C652 (2011).
[48]D. Verma, F. Meng, F. Sachs, and S. Z. Hua, "Flow-induced focal adhesion remodeling mediated by local cytoskeletal stresses and reorganization," Cell Adhes. Migr. **9**, 432–440 (2015).
[49]M. Essig, F. Terzi, M. Burtin, and G. Friedlander, "Mechanical strains induced by tubular flow affect the phenotype of proximal tubular cells," Am. J. Physiol. Renal Physiol. **281**, F751–F762 (2001).
[50]A. K. O'Connor *et al*., "An inducible CiliaGFP mouse model for in vivo visualization and analysis of cilia in live tissue," Cilia **2**, 8 (2013).